Fragmentation and multifragmentation of 10.6*A* GeV gold nuclei

M. L. Cherry,[2] A. Dabrowska,[1] P. Deines-Jones,[2] R. Holynski,[1] W. V. Jones,[2] E. D. Kolganova,[3] A. Olszewski,[1] K. Sengupta,[2] T. Yu. Skorodko,[3] M. Szarska,[1] C. J. Waddington,[4] J. P. Wefel,[2] B. Wilczynska,[1] B. Wosiek,[1] and W. Wolter[1]

(The KLMM Collaboration)

[1]*Institute of Nuclear Physics, Kawiory 26A, 30-055 Krakow, Poland*
[2]*Department of Physics and Astronomy, Louisiana State University, Baton Rouge, Louisiana 70803*
[3]*Institute of Theoretical and Experimental Physics, B. Cheremushkinskaya 25, 117-259 Moscow, Russia*
[4]*School of Physics and Astronomy, University of Minnesota, Minneapolis, Minnesota 55455*

(Received 22 June 1995)

Interactions of 10.6*A* GeV gold nuclei have been studied in nuclear emulsions. In a minimum bias sample of 1100 interactions, 4730 helium nuclei and 2102 heavy nuclei were emitted as fragments of the incident gold projectiles. The emission angles of these fragments have been measured and pseudorapidity distributions constructed. The multiplicity distributions have been considered separately for the light and heavy target nuclei in the emulsions and found to be relatively independent of the nature of the target, when studied in terms of the total charge remaining bound in the multiply charged fragments. These distributions have been compared with those reported by experiments that studied the multifragmentation of 0.6 and 1.0*A* GeV gold nuclei, and show relatively small but statistically significant differences that may be attributed to the differing energies or, possibly, to detection biases in the low energy data. We have also looked for evidence of phase changes in the description of multifragmentation and compared our conclusions with those of a study of 1.0*A* GeV gold nuclei interacting in a carbon target. We see evidence of behavior that is similar, but not entirely consistent, with that reported at the lower energy. Whether this is evidence for a true phase change in the state of the nuclear matter remains an open question.

PACS number(s): 25.75+r, 29.40.Rg

I. INTRODUCTION

Studies of the interactions of high energy heavy nuclei with target nuclei have become much easier with the availability of beams of such nuclei from accelerators. Initially such studies either depended on examining the interactions of comic ray nuclei, which were essentially limited by flux considerations to nuclei of iron and lighter, or attempted to analyze the fragments produced from stationary target nuclei bombarded by high energy nucleons. When the nucleus whose disruption is being studied is moving, then the fragments produced will also be moving and can be more readily identified than if they are emitted from a stationary nucleus. The experiment to be described here examines the breakup of relativistic gold nuclei when they interact with the target nuclei in nuclear emulsions. The fragments produced are readily identified in the emulsions. Specific attention in this paper is directed towards the multiply charged fragments that are produced. Other features of these interactions, such as the production of mesons and other unstable particles, will be addressed elsewhere.

In relatively peripheral collisions between nuclei, the major part of the projectile nucleus is not directly involved in the interaction, but is left in a highly excited state. This excited piece of nuclear matter then loses its energy by breaking up into a few or many fragments. The relative yields of the different types of fragment and the relationships between them are measures of processes that occur during the breakup of these excited nuclear remnants. In this paper we will study some of these relationships and compare them with those observed for similar projectiles interacting with energies an order of magnitude less than that used in this experiment.

II. EXPERIMENT

The interactions of gold nuclei accelerated by the Brookhaven AGS have been studied by using nuclear emulsions as both the target and detector. These gold nuclei had an incident energy of 10.6*A* GeV and were recorded in several small stacks of emulsion oriented so that the pellicules lay along the beam axis. Thus the tracks of individual nuclei were generally confined to a single pellicule and could be readily traced from the point of entry to an interaction or to the point of exit from the analysis volume. Interactions were located using a microscope scan across the top edge of each pellicule to locate the tracks of incoming gold nuclei. These tracks were then followed down through the pellicule under high magnification until an interaction was detected or the track reached the end of the microscope travel. Each interaction detected in this manner was then analyzed in detail. Preliminary reports on the main characteristics of these interactions have been published previously [1–3].

Three classes of particles are observed in the interactions observed in emulsions, fragments of the target nucleus, fragments of the projectile nucleus with $Z \geq 2$, and fast singly charged particles, which includes particles produced in the nucleon-nucleon interactions, mostly π mesons. At these high projectile energies these different classes of particles can generally be readily distinguished, although it is not possible to separate the produced particles and the singly charged fragments from the projectile, which both appear as forwardly directed tracks having minimum ionization. The

singly charged fragments from the projectile will include both spectator and participant particles. As a result this experiment is unable to study the singly charged fragments on a particle by particle basis, although the number of such particles can be derived from charge conservation considerations. The majority of the fragments from the target nucleus have relatively low energies and produce black and gray tracks with an angular distribution that for the black tracks is approximately isotropic, but which is peaked forward for the gray tracks. In general, it is not possible to assign a charge to the black tracks, while the gray tracks are essentially all singly charged and are known to include all three isotopes of hydrogen and an occasional produced particle [4]. The black tracks can be regarded as being exclusively produced by particles emitted from the target nucleus, whereas some of the gray tracks could be due to projectile particles that have lost most of their energy in the interaction. For these massive and high energy projectiles incident on relatively light target nuclei, this is less likely than at lower energies, but there is also the possibility that some of the target nucleons are swept up by the projectile and appear as fast particles that are indistinguishable from the projectile singly charged fragments.

The emulsions represent a composite target with three main constituents: relatively heavy nuclei of Ag and Br (45% by cross section), light nuclei of C, N, and O (35%), and hydrogen (20%). We observed previously [5] that for these high energy gold projectiles there is a rather clean separation between two classes of interactions, those with heavy (Ag, Br) and those with light (H, C, N, O) targets. We estimate that the target assignments are correct for at least 95% of all the interactions.

The multiply charged fragments of the projectile must emerge from the interactions with essentially the same energy per nucleon as the incoming projectile, although some of the singly charged particles, if they are not "spectator protons," may have suffered significant energy losses. The multiply charged fragments can be readily identified as fragments, and their charges can be determined from the nature of the tracks. The total numbers of alpha particles, n_α, and of fragments with $Z \geq 3$, n_Z, can be determined for each interaction. The total number of multiply charged fragments, m_F $(=n_\alpha+n_Z)$, is then an indication of the degree of multifragmentation occurring in an interaction and provides the main topic to be addressed in this paper. The emission angles of each fragment with respect to the initial direction of the projectile can be measured with considerable accuracy. Consequently the transverse momentum imparted to each fragment can be deduced by assuming that the total momentum is unchanged in the interaction.

It is convenient, in order to compare our results with other experiments, to organize the interactions in terms of the projectile charge that remains bound after the interaction in the form of multiply charged fragments, Z_b. This quantity is then assumed to be an indicator of the degree of breakup or "centrality" of the interaction. Models of nucleus-nucleus interactions suggest that Z_b is closely correlated to the impact parameter [6]. The bound charge can also be regarded as a measure of the size of the residual nucleus left from the projectile after the initial interaction. Experiments that are unable to detect with high efficiency the copious numbers of helium nuclei emitted in these interactions cannot reliably evaluate Z_b. The correlation between Z_b, computed including the alphas, and Z_b^*, computed without alphas, covers a band of charges 10–15 charge units wide, showing that Z_b^* is a poorer measure of the impact parameter than that obtained when the alphas can be included. Presumably a measure of Z_b that also included the $Z=1$ spectator nuclei would be a still better measure of the impact parameter, but these cannot be reliably distinguished from other singly charged particles in these experiments.

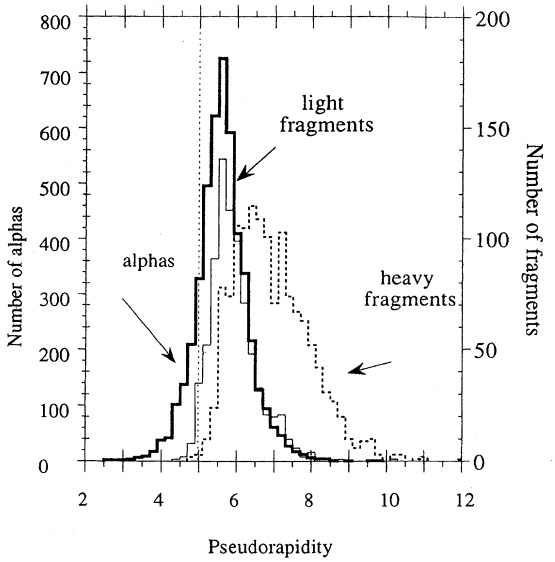

FIG. 1. Pseudorapidity distributions for alpha particles, heavy line, light ($3 \leq Z \leq 5$), thin line, and heavy ($Z \geq 6$) dashed line, fragments. Also shown as a vertical dashed line is the 95% acceptance value quoted by the ALADIN array for light fragments. Note differing scales for alphas and heavier fragments.

Multifragmentation of gold nuclei at lower energies was originally studied at the Bevalac in nuclear emulsions by Waddington and Freier [7]. However, these studies had relatively small statistics and were for nuclei which came to rest in the emulsions and hence included interactions over the whole energy range from $1.0A$ to $0A$ GeV. More extensive results have been reported since for gold nuclei with $0.6A$ GeV interacting in targets of C, Al, Cu, and Pb, using the ALADIN forward spectrometer at GSI [6,8], by the EOS Collaboration for $1.0A$ GeV gold nuclei interacting in various targets [9–11] and by etchable plastic detectors [12]. Here we will compare the results from these low energy gold nuclei with those obtained at $10.6A$ GeV by us in emulsions.

The ALADIN array is stated to have an acceptance that would allow the detection of more than 95% of the fragments with $Z \geq 3$ and a discriminator threshold low enough to detect charges of helium and heavier. However, since the alphas typically have a distribution in pseudorapidity that extends to lower values than does the distribution for even the lightest heavier fragments, as can be seen in Fig. 1, this acceptance limit implies that a significant fraction (15–20 %) of the helium nuclei will have been missed. While general corrections can be made for such losses if they are understood, they cannot be made on an event-by-event basis. Consequently, estimates of Z_b for individual interactions will

tend to be too low, although not by an amount sufficient to explain the differences between the ALADIN and our data (e.g., Fig. 11). For fragments with $Z \leq 8$ individual charges were resolved, while the resolution deteriorated to a full width at half maximum (FWHM) of ± 2.0 for heavier fragments, which is comparable to the resolution obtainable in emulsions.

The EOS experiment essentially detected and identified all particles emitted forward from interactions [11]. The plastic detectors [12] were limited to the detection of nuclei with $Z \geq 6$ and hence, as we will see below, were unable to detect the majority of the multiply charged fragments emitted in these interactions. For comparison the emulsions detected 100% of the heavier fragments as well as all the singly charged particles. The ALADIN results were taken on several discrete targets and hence could study any target dependence directly. As we shall see, most of the variables to be discussed show little if any dependence on the target when the interactions are considered in terms of Z_b.

The detection efficiencies of minimum bias scans in nuclear emulsions can vary considerably depending on the human factors involved. In this experiment, two independent scans were made, one at Minnesota and the other at Krakow, with results that were very consistent. In all, 2412 charge-changing interactions were detected (of which a random sample about 1100 were analyzed for this paper). The mean free path, $\lambda_{\rm em}(cc)$, obtained from this sample was 4.67 ± 0.10 cm, which is significantly smaller than that reported by another emulsion experiment [13]. Our measured value can be compared with the mean free path calculated for emulsion from the directly measured cross sections for charge-changing interactions in a wide range of targets for the same gold beam. These cross sections were determined by an array of electronic detectors [14–16] and by etchable glass detectors [17]. When these measured cross sections are used to verify the hard sphere models of Binns *et al.* [18] and Westfall *et al.* [19] developed to represent the nuclear cross sections, values for the cross sections can be calculated for all the elements in the emulsion. From these a value of $\lambda_{\rm em}(cc) = 4.25 \pm 0.1$ cm can be deduced for charge changing interactions in emulsion.[1] This is less than the mean free path measured by us for all the observed charge-changing interactions and suggests that either many of the interactions detected in the emulsion with no apparent charge change, and thus not included in $\lambda_{\rm em}(cc)$, did indeed involve small charge changes, or that some 9% of all the charge changing interactions have been missed. The electronic measurements suggest that some 9–11 % of the interactions should be due to interactions with very small charge changes, $\Delta Z = -1$ or -2, whereas only about 7% of all the interactions found in the emulsions have such small charge changes. Any missed interactions in our samples must have been characterized by negligible charge changes and modest particle production. Hence their absence should not significantly affect the studies of multiple fragmentation discussed here. At most they would result in a small systematic change in the absolute rates derived for various yields.

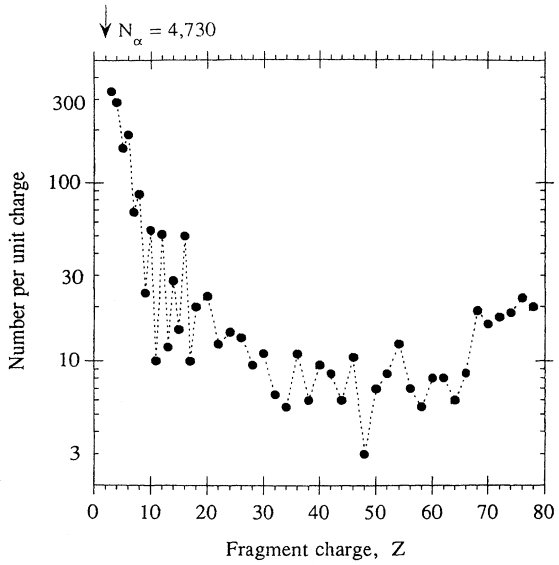

FIG. 2. The charge distribution of the fragments emitted from 1100 charge changing interactions.

The charge distribution of the 2102 fragments with $Z \geq 3$ emitted from all the interactions analyzed in the emulsions is shown in Fig. 2. This distribution is characterized by a strong peak with 964 light fragments, those with $Z \leq 6$. For comparison, the total number of helium nuclei emitted was 4730, and clearly the number of these nuclei dominates those of any other fragment. Apart from the peak of low Z nuclei, this distribution is very similar to that reported by the plastic nuclear track detectors [12]. It can be noted that there is no significant evidence for any fission produced enhancement in the $35 \leq Z \leq 45$ region of the distribution, such as that seen at lower energies. This is further confirmation of the previously reported almost total lack of fission of gold at these high energies [1–3].

III. FRAGMENTS WITH $Z \geq 2$

The general features of the fragmentation of the projectile can be summarized by comparing the yields of alpha particles with that of heavier ($Z \geq 3$) fragments. An area plot of the correlation between n_α and n_Z is shown in Fig. 3. This figure shows that the number of pure central interactions, those with both n_α and $n_Z = 0$, is very small ($\approx 1\%$), while the numbers of those with just one $Z \geq 3$ fragment but few or no alphas are large. It also shows that a considerable proportion of the interactions have multiple $Z \geq 3$ fragments. Those events lying above the diagonal line on Fig. 3 had more than five $Z \geq 2$ fragments, while there was one event with 19 fragments, 15 alphas, and $4Z \geq 3$ fragments. An indication of the relation between the charges of the $Z \geq 3$ fragments is illustrated in Fig. 4, which is an area plot of the correlation between the charge of the heaviest fragment, Z_1, and the next heaviest, Z_2. The physical restrictions are indicated by the dotted lines on this plot, but it is clear that the allowed space

[1]The uncertainty on this value is difficult to evaluate reliably, since the cross sections used are determined from models. However, these models have been derived from experimental cross sections that have uncertainties significantly less than 1%, and so an uncertainty of 2% or ± 0.1 cm appears reasonable.

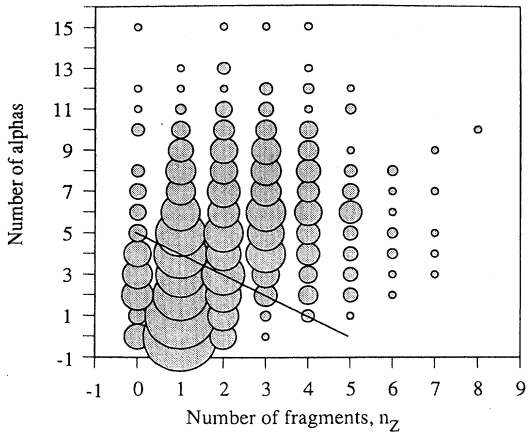

FIG. 3. Correlation between number of fragments, n_Z, and number of alpha particles, n_α. The number of interactions in each class is proportional to the area of the circle. Events above the diagonal line had $m_F \geq 6$.

is not uniformly populated. In particular, the fission region near the apex is almost empty, in contrast to the situation seen at lower energies by plastic detectors [12]. The lower limit on detection by these plastic detectors is indicated by the horizontal dashed line on this plot.

A. Leading fragments

From Fig. 4 it can be seen that there are no interactions for which there was a fragment with $Z \leq 66$ and no other multiply charged particle emitted. Figure 4 can be compared with a plot of the correlation between Z_1 and the sum of the remaining bound charge, Z_r, Fig. 5. This shows that there are many interactions where $Z_r > Z_1$ and that, even when there is a well-defined leading fragment—that is, a fragment that carries more than half of the bound charge—it is usually

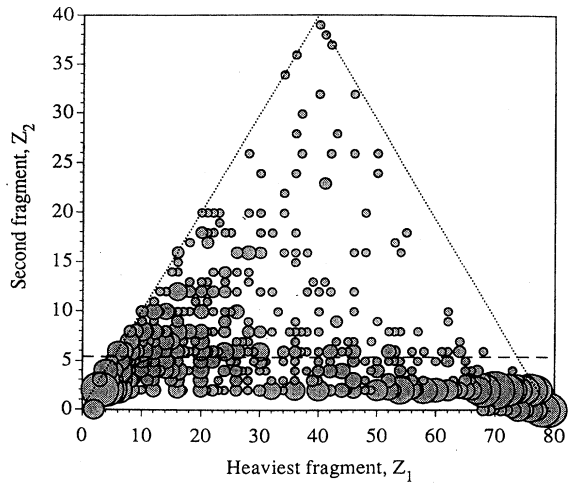

FIG. 4. Correlation between heaviest, Z_1, and second heaviest, Z_2, fragments. Diagonal dashed lines show physical limits. Horizontal dashed line shows lowest detection limit of plastic detectors.

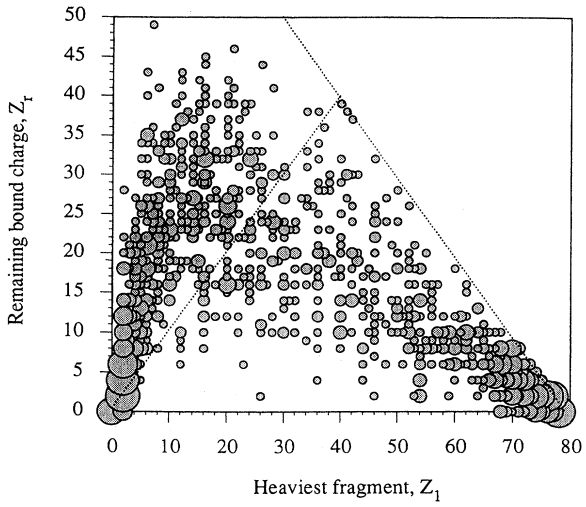

FIG. 5. Correlation between charge on heaviest fragment, Z_1, and remaining bound charge Z_r. Right diagonal dashed line shows charge limit, left shows where $Z_r = Z_1$.

accompanied by appreciable other bound charge. A similar comparison can be drawn from the correlation between Z_2 and Z_3, which indicates that there are very few interactions with two $Z \geq 3$ fragments that are not also accompanied by at least an alpha particle.

As Z_b decreases there is a marked change in the characteristics of the fragmentation of the residual nucleus. For large Z_b, >60, there is generally a well-defined leading fragment. The fraction of the total bound charge that is carried by this leading fragment falls sharply with decreasing Z_b. Consider the ratio R, for all fragments, where

$$R = \frac{Z_1}{\sum_{i>1} Z_i + 2n_\alpha} = \frac{Z_1}{Z_r} \tag{1}$$

and Z_1 is the heaviest fragment emitted from the interaction. Then there is a leading fragment, as defined above, when $R > 1.0$. R is a strong function of Z_b. Thus, while there is a well-defined leading fragment when $Z_b \approx 65$, it is much less well defined when Z_b falls to ≈ 35. For example, Fig. 6 shows the mean value of R, $\langle R \rangle$, in several bins of Z_b where $\langle R \rangle$ varies rapidly with Z_b. This plot suggests that at about $Z_b \approx 50$ only half of the interactions have a leading fragment, $\langle R \rangle = 1.0$, while by $Z_b \approx 70$ most, if not all, have a leading fragment. Apparently it is difficult to induce multifragmentation in interactions where most of the matter remains bound after the initial interaction.

The mean charge on the heaviest fragments, which are not necessarily leading fragments as defined above, $\langle Z_1 \rangle$, is correlated with Z_b, as can be seen in Fig. 7. Also shown are results from ALADIN at 0.6A GeV, which can be seen to be significantly different from our results at high energy. However, these differences could be partially accounted for by the systematic underestimation of Z_b in the low energy results due to the missing of helium nuclei, and it is premature to conclude that they represent a true energy dependence. In both cases it is clear that $\langle Z_1 \rangle$ is always much less than Z_b,

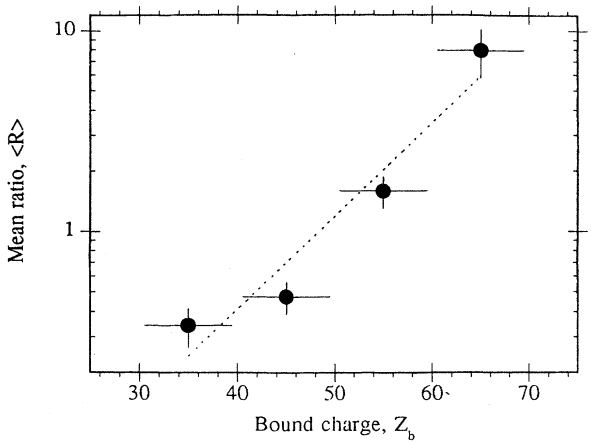

FIG. 6. Mean values of the leading fragment ratio $\langle R \rangle$, Eq. (1), as a function of bound charge, Z_b. An exponential fit is shown to guide the eye.

although the two approach at the highest values, where the influence of helium nuclei on the estimates of Z_b would be reduced.

B. Intermediate mass fragments (IMF's)

Mean values of the multiplicities of fragments in these interactions, $\langle n_Z \rangle$ and $\langle n_\alpha \rangle$ as determined in small intervals of Z_b, for the "heavy" and "light" targets in the emulsions are shown separately in Fig. 8. It can be seen that both means have a maximum at intermediate values of Z_b and fall off for both large and small Z_b. The only indication of a statistically significant dependence on the type of target is for $60 \leqslant Z_b \leqslant 70$. The shapes of the distributions, as indicated by the two third order polynomials fitted to the light target data

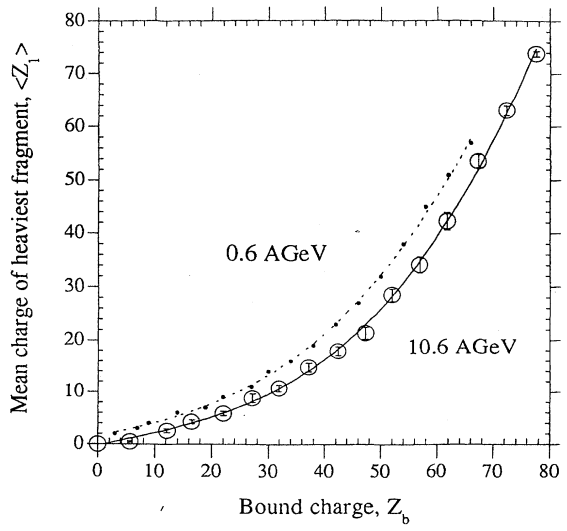

FIG. 7. Mean values of the leading charge $\langle Z_1 \rangle$ as a function of the bound charge, Z_b, at high energy emulsion data, solid line, and low energy ALADIN data, dashed line [8].

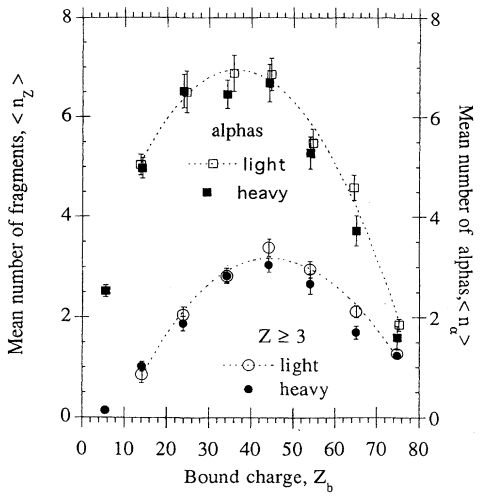

FIG. 8. Mean number of fragments, $\langle n_Z \rangle$, left hand, and alphas, $\langle n_\alpha \rangle$, right hand, as a function of the bound charge, Z_b. Values for light and heavy targets are shown as open and solid symbols, respectively. Curves are fitted to the light values to guide the eye.

to guide the eye, are basically similar but differ in detail. The helium distribution peaks at a lower value of Z_b than does that of the heavier fragments.

Neglecting any residual target dependence, we can combine the data to study the multiplicities in more detail. The mean $Z \geqslant 2$ fragment multiplicity, $\langle m_F \rangle$, has its greatest values for $30 \leqslant Z_b \leqslant 49$, and this is clearly the region where multifragmentation is the dominant mode of disassembly of the projectile. The distributions in m_F and n_Z for these interactions are shown in Fig. 9. This figure shows that m_F ranges between 2 and 19 with a maximum at 9–11, while n_Z has a maximum at 3, but can be as great as 7. These values can be compared with those for the whole sample seen in Fig. 3. The relative yields of these $Z \geqslant 3$ fragments depend quite significantly on Z_b. The probabilities that fragments lying within small charge intervals should be emitted from an in-

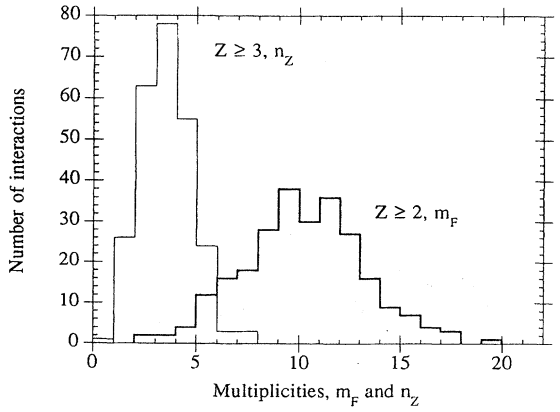

FIG. 9. Distributions, for interactions with $30 \leqslant Z_b \leqslant 49$, of the multiplicities for all $Z \geqslant 2$ fragments, m_F, and for $Z \geqslant 3$ fragments, n_Z.

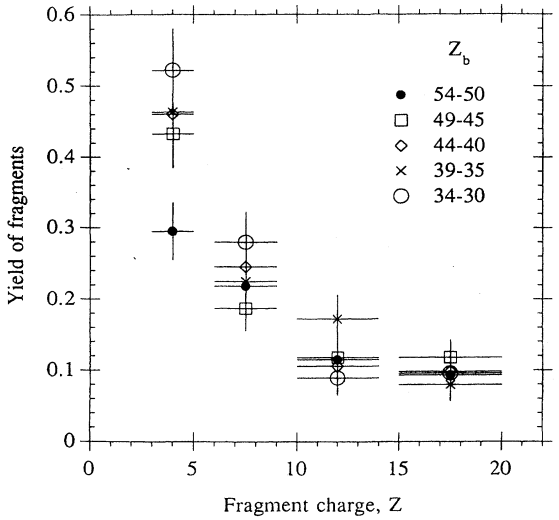

FIG. 10. Yields of fragments in narrow charge intervals for various values of the mean bound charge.

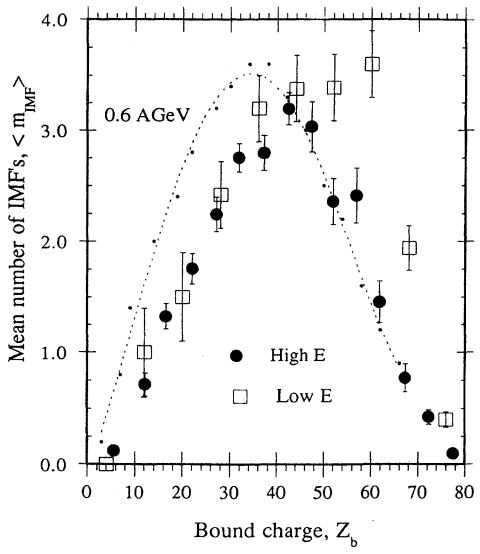

FIG. 11. Mean values of IMF multiplicities, $\langle m_{\mathrm{IMF}} \rangle$, as a function of bound charge, Z_b, from emulsions at 10.6 and $<1.0A$ GeV [7]. Also shown are results for 0.6A GeV gold projectiles from the ALADIN array [15] fitted with a smooth curve to guide the eye.

teraction are shown in Fig. 10 for several intermediate intervals of Z_b. It can be seen that while the yield of fragments with $15 \leq Z \leq 20$ is almost independent of Z_b in this range, it nearly doubles for the lightest fragments with $3 \leq Z \leq 5$ as Z_b decreases from the low 50's to the low 30's. The $Z=2$ nuclei also show mean multiplicities over this range of Z_b that follow a similar trend: see Fig. 8. This suggests that the emission of helium nuclei is not a fundamentally different process than that of the slightly heavier nuclei.

Intermediate mass fragments (IMF's) were defined by the ALADIN group as being those fragments with $3 \leq Z \leq 30$, thus excluding the helium nuclei. These authors showed that the multiplicity of the IMF's, when averaged over small intervals of Z_b, $\langle m_{\mathrm{IMF}} \rangle$, was well organized by Z_b. A representation of a universal curve for all four targets studied in the ALADIN work is shown in Fig. 11 as a dashed line. In fact there is a slight indication, both from these results and in our own study, that for high Z_b values, at and above the peak in $\langle m_{\mathrm{IMF}} \rangle$, the lighter targets produce larger values of $\langle m_{\mathrm{IMF}} \rangle$ than do the heavier targets. Also shown in Fig. 11 are our values in emulsion of $\langle m_{\mathrm{IMF}} \rangle$ for all targets for both the $10.6A$ GeV and $<1.0A$ GeV [7] samples. It can be seen that at high energy we observed significantly fewer IMF's at small values of Z_b than was seen at the lower energies of the ALADIN experiment. However, when we compare these high energy results with those from the earlier low energy emulsion study, we see remarkably good agreement for $Z_b \leq 50$, in spite of the lower statistical weight of these old results. There is a clear disagreement between the low energy emulsion data with that from ALADIN, even though they are nominally at similar energies. These comparisons suggest that the differences with the ALADIN results cannot be entirely attributed to the underestimations of Z_b due to the failure to detect all of the alpha particles. If we consider the emulsion results alone, it appears that the only significant energy-dependent difference that might be present is for $Z_b \geq 50$, where the emulsion results show that $\langle m_{\mathrm{IMF}} \rangle$ is appreciably greater at low than at high energies. This observation must be tentative, since for high Z_b the ALADIN values agree well with the high energy emulsion data, and one would expect that the influence of the alphas would be reduced.

The helium nuclei are the numerically dominant fragments emitted from these interactions. The mean numbers of helium nuclei for all the high energy interactions, $\langle n_\alpha \rangle$, are shown in Fig. 12 as a function of Z_b and compared with $\langle m_{\mathrm{IMF}} \rangle$ values for light ($Z \leq 6$) and heavy ($6 < Z \leq 30$) IMF's.

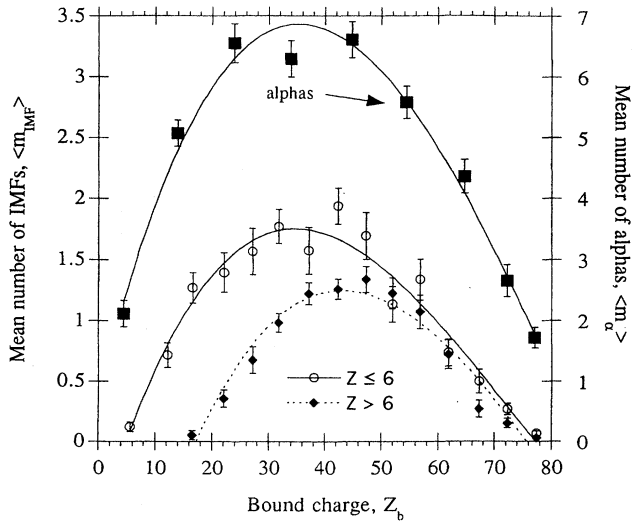

FIG. 12. Mean multiplicities for light ($Z \leq 6$) and heavy ($6 > Z \leq 30$) IMF's, left-hand scale, and alphas, $\langle n_\alpha \rangle$, right-hand scale, as a function of bound charge, Z_b. Third order polynomials are fitted to each class to guide the eye.

It is apparent that the alphas and light IMF's have an appreciably wider spread than the heavier IMF's, with copious production for quite small values of Z_b. This suggests that even quite small residual nuclei can still emit appreciable numbers of these light nuclei, whereas it is physically impossible for them to emit appreciable numbers of heavier fragments. In every case it is clear that multifragmentation is most significant for intermediate residual nuclei, with Z_b between 30 and 50, when $\langle n_\alpha \rangle$ is between 6 and 7 and $\langle m_{\mathrm{IMF}} \rangle$ is about 3, so that such events are characterized on average by the emission of some ten multiply charged fragments.

IV. MOMENTS OF CHARGE DISTRIBUTIONS

It has been suggested by Campi [20] that the ith moments of the charge distributions provide a test of the suggestion that multifragmentation can be described in terms of percolation theory. The ith moments of the charge distribution of the n multiply charged fragments in a single event are given by

$$M_i = \sum_{n-1} Z_n^i , \tag{2}$$

where the sum is extended over all multiply charged fragments in an interaction apart from the heaviest fragment, which is regarded as the "percolating" cluster. Here M_0 is the number of additional multiply charged fragments, $m_F - 1$, and M_1 $(=Z_r)$ is the total charge of these fragments. Thus, in terms of defined quantities,

$$Z_b = Z_1 + M_1 . \tag{3}$$

The plot of Z_1 versus M_1, already presented as Fig. 5, shows a clear, but complex correlation, which suggests two distinct populations. This suggestion can be enhanced by separating the interactions into those with and without a leading fragment, i.e., where Z_1 is $>$ or $<$ than M_1. As we shall see later, Sec. V, this separation is somewhat analogous to that found from a consideration of the possibility that there is a phase change in the nuclear matter with increasing multiplicity. If the mean values of Z_1, $\langle Z_1 \rangle$, are determined over small intervals of M_1, then these two classes are illustrated in Fig. 13, which shows a clear separation between them.

The mean values of M_0, M_1, and M_2, averaged over small ranges of Z_b for nonzero values of the moments, are shown as functions of Z_b in Fig. 14. It should be noted that the values for the highest bin in Z_b are seriously distorted by the four clean fission events that were observed. Removing these from this sample changes the mean value of M_2 in this bin from 38.5 to 13.2. The correlation between $\langle M_1 \rangle$ and $\langle M_2 \rangle$, shown in Fig. 15, results in a hysteresis loop that proceeds clockwise with decreasing $\langle Z_b \rangle$ and is an indication of the asymmetric nature of the two distributions.

Normalized moments S_n can be defined by dividing by M_1:

$$S_n = M_n / M_1 . \tag{4}$$

It was also suggested by Campi [20] that if there is some critical behavior in the breakup of the nuclei, such as a liquid-gas phase transition, then some events should have values of S_n much larger than the average. In particular, it was shown that for the low energy gold interactions [7] there was a wide range of values and strong and approximately linear correlations between the different normalized moments, although it was not possible to conclude that there was a phase transition. Very similar correlations over a similar range of values are found for the much higher energy gold interactions reported here, Fig. 16. Here, again, it is not possible to conclude from these results that there was a phase transition. These correlations are essentially unaffected if the analysis is restricted to those interactions that are clearly cases of multiple fragmentation by only including those with

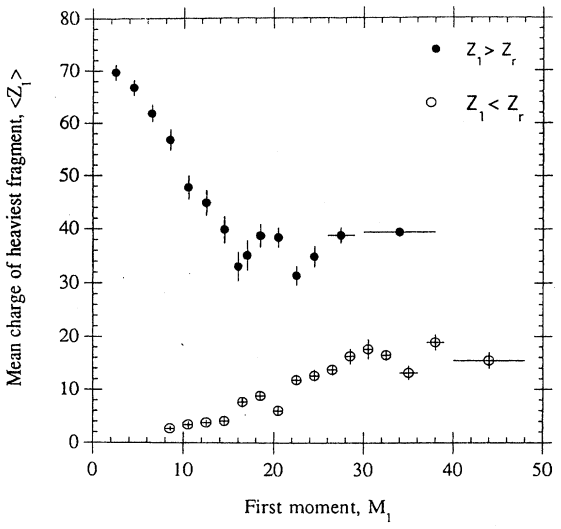

FIG. 13. Mean values of the charge on the heaviest fragment, $\langle Z_1 \rangle$, as a function of the first moments, M_1, separated into those events where Z_1 is $>$ or $<$ than M_1 $(=Z_r)$.

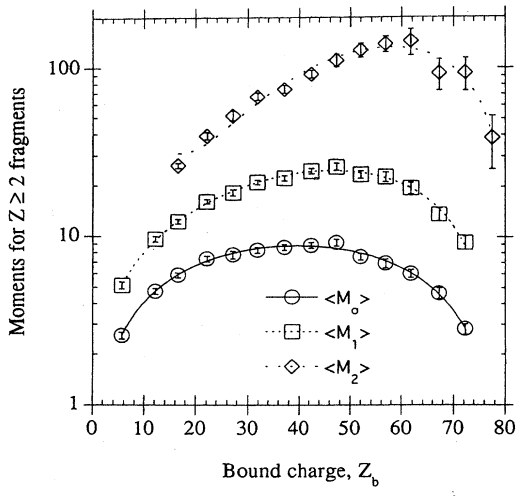

FIG. 14. Zeroth, first and second moments, Eq. (2), as a function of bound charge, Z_b. In each case a third order polynomial has been fitted to guide the eye.

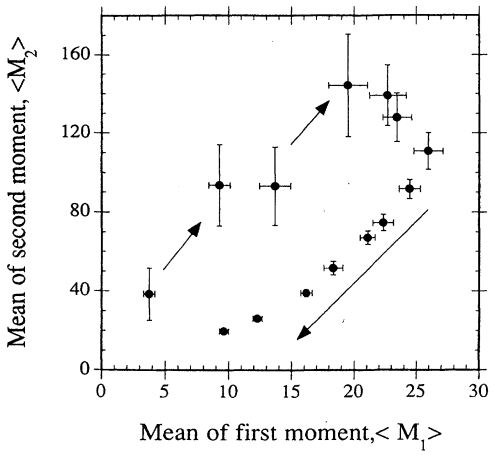

FIG. 15. Correlation between mean values of first, $\langle M_1 \rangle$ and second, $\langle M_2 \rangle$, moments, in intervals of Z_b, with Z_b decreasing from the lower left.

two or more IMF's. Apart from a reduction in the number of events, the only significant differences are in the removal of a few with the highest values of S_n. Similarly these correlations and the range of values covered are unaffected by the presence or absence of a leading fragment. The clear curvatures observed in these correlations have been attributed by Campi to the finite size of the nuclei, but the approximate slopes are close to those expected from percolation models, which would predict a linear correlation between these parameters.

Two particular combinations of these moments can be considered in terms of Z_b: S_2 from Eq. (4) and

$$\gamma_2 = M_2 M_0 / M_1^2, \tag{5}$$

and the mean values of these combinations, binned over Z_b,

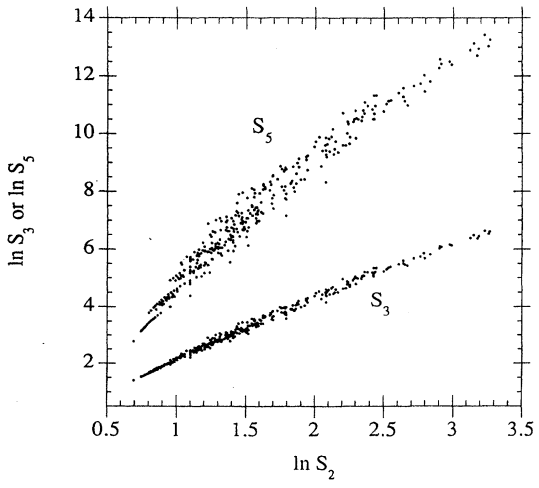

FIG. 16. Plots of $\ln S_3$ and $\ln S_5$ as a function of $\ln S_2$ for almost all interactions, with S_i defined by Eq. (4) (see text).

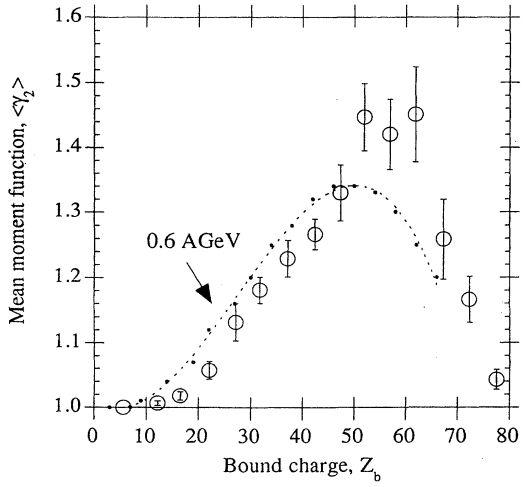

FIG. 17. Variations of the mean values of the second combination of moments, γ_2, as defined by Qu. 5, with bound charge, Z_b, for our data and the ALADIN [15] results at 0.6A GeV.

can be determined. Both $\langle S_2 \rangle$ and $\langle \gamma_2 \rangle$ have their maximum values for $50 < Z_b < 65$ and fall off rather steadily for lower values of Z_b.

The second combination of moments γ_2 can also be expressed as the normalized charge variance [8]

$$\gamma_2 = \frac{\sigma_e^2}{\langle Z \rangle_e^2} + 1, \tag{6}$$

where σ_e^2 is the variance of the charge distribution of the fragments, other than the heaviest, in an interaction, and $\langle Z \rangle_e$ is the mean charge of these fragments. Thus $\gamma_2 = 1$ if all the charges of these fragments are the same, while a large value implies a wide range of charges for these fragments. A comparison of the values of $\langle \gamma_2 \rangle$ at 0.6A and 10.6A GeV, plotted as a function of Z_b, Fig. 17, shows features closely similar to those seen in Fig. 11. There is a small, but apparently significant reduction in $\langle \gamma_2 \rangle$ at high energies for $Z_b \leq 45$, but for $45 \leq Z_b \leq 65$ the high energy values of $\langle \gamma_2 \rangle$ are considerably larger than those at low energy. In this region it appears that at high energy when there is a relatively large residual nucleus the interactions have more channels into which to fragment and thus there is a wider range of charges emitted. Examination shows that γ_2 has a considerable dispersion for large Z_b but that this is rapidly reduced as Z_b decreases. It is also found that small values of γ_2 are favored, even at large values of Z_b.

V. CRITICAL EXPONENTS IN MULTIFRAGMENTATION

The EOS collaboration [9] have recently reported some of their results from the analysis of 1.0A GeV gold nuclei fragmenting in a carbon target. In this experiment it was possible to detect and identify nearly all the charged reaction products on an event-by-event basis. In particular, they were able to determine, for each interaction, the multiplicity m for both singly and multiply charged particles. In their analysis of data from 9716 interactions they used "the methods devel-

oped for determining percolation critical exponents to extract the critical exponents for nuclear matter from the moments of the fragment charge distribution." A discussion of this analysis [21] has suggested that these results do not unambiguously identify the exponents that are determined as being representative of critical phenomena. Nevertheless, it is clearly interesting to compare the EOS analysis with one based on our data.

The EOS group assumed that the multiplicity of fragments, m ($=m_F$+No. of released protons), is a linear measure of the distance from the critical point, as suggested by Campi [20]. The region in m below the assumed critical multiplicity m_c is designated as the "liquid" phase and that above m_c as the "gas" phase. It is assumed that in the liquid phase the heaviest fragment Z_1 is omitted in forming the moments, but is not omitted when in the gas phase. It should be emphasized that in this analysis the moments used include the $(79-Z_b)$ protons as fragments, modifying Eq. (2) and replacing M_i by M_i^*. The analysis by Gilkes *et al.* [9] states that the critical exponents for large systems are given in terms of the multiplicity difference, $m-m_c=\zeta$, by

$$M_2^* \sim |\zeta^{-\gamma}|, \tag{7}$$

$$Z_1 \sim |\zeta|^{\beta}, \tag{8}$$

$$n_Z \sim Z^{-\tau} \quad \text{for } m=m_c. \tag{9}$$

These exponents are known [22] to be related by

$$\tau = 2 + \frac{\beta}{\beta+\gamma}. \tag{10}$$

These authors then used the second moments to determine the critical multiplicity by adjusting the assumed value of m_c until the exponent γ in Eq. (7) was the same in both the gas and liquid phases. This procedure is somewhat subjective, since the values of γ depend quite strongly on the range of ζ selected, particularly in the liquid phase. Nevertheless, these authors report a value for $m_c=26\pm1$ with a mean value for γ of 1.4 ± 0.1.

Even though our statistics are nearly an order smaller than those from the EOS experiment and our interactions are with a range of targets, we have studied projectiles with an order of magnitude greater energy. It appears worthwhile to attempt a similar analysis to look for similar signs of critical behavior in our data set. We begin by examining the variation of the mean second moments, including the protons as determined by charge balance considerations, $\langle M_2^* \rangle$, for each interval of m, with Z_1 removed in every case. A plot of $\langle M_2^* \rangle$ as a function of m is shown in Fig. 18. In order to reduce the effects of the large fluctuations produced at small values of m by interactions with two large fragments, we removed events with values of $M_2^* > 5x\langle M_2^* \rangle$ in that m bin. The 14 events removed all had $m<20$. The effects of these fluctuations could also be reduced by considering the means of $\ln M_2^*$ rather than the logarithm of mean M_2^*, but this distorts the derived exponents. A relatively abrupt change in this distribution is apparent for $m \approx 26$, suggesting that there could be a phase change at this critical value of m_c. This value is similar to that reported at 1.0A GeV in spite of our

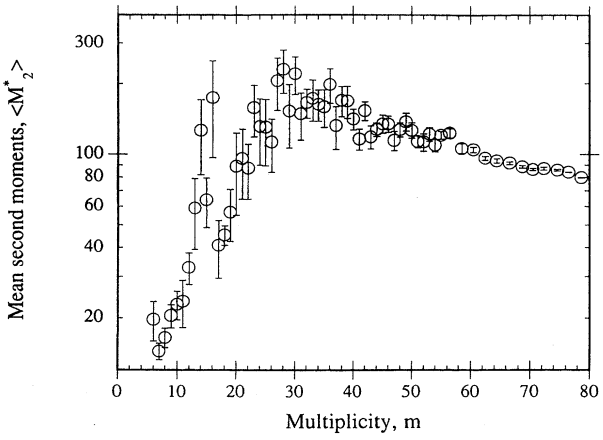

FIG. 18. Mean second moments $\langle M_2^* \rangle$ as a function of multiplicity m.

assumption that all the released protons are fragments, i.e., spectators, which should lead to an overestimate of the true number of such fragments.

Following the example of Gilkes *et al.* [9], Fig. 19 shows a log-log plot of $\langle M_2^* \rangle$ with $|\zeta|$ for the assumed liquid and gas phases, setting $m_c=26$. The clear separation between the two phases arises from the inclusion of Z_1 in the determinations of $\langle M_2^* \rangle$ in the gas phase. When examined over the entire available range of $|\zeta|$, neither phase shows the power law behavior predicted by Eq. (7). However, if rather narrow regions of $|\zeta|$ are selected, Fig. 20, then a good fit to such a power law can be obtained for the gas phase, with $\gamma_{\text{gas}}=0.57\pm0.05$ and a reduced χ^2 of 1.36. This value is relatively insensitive to the range of $|\zeta|$ used. A fair fit can also be obtained for the liquid phase, but with a significantly different exponent. The relative insensitivity of the exponent γ_{liquid} to the range of $|\zeta|$ is illustrated by noting that adding two more higher values of $|\zeta|$ to those shown in Fig. 20 changes γ from 1.12 ± 0.12, with a reduced χ^2 of 2.5, to 1.27 ± 0.09, while removing the two highest values shown

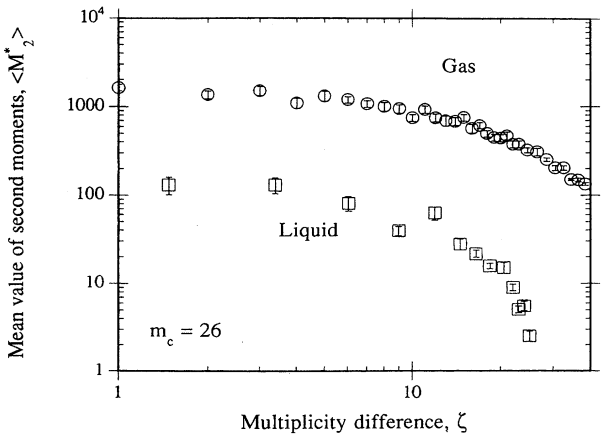

FIG. 19. Mean second moments $\langle M_2^* \rangle$ as a function of the multiplicity difference ζ assuming $m_c=26$.

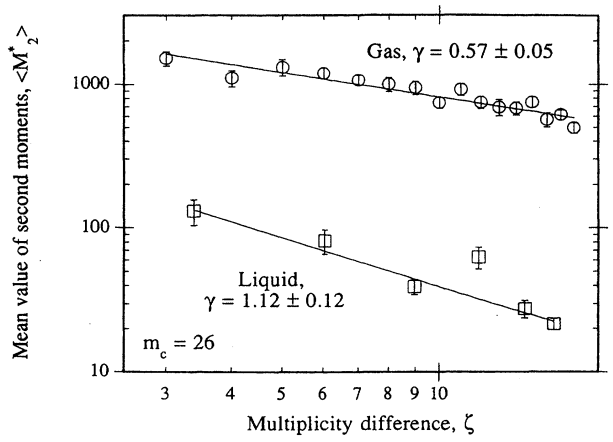

FIG. 20. Mean second moments $\langle M_2^* \rangle$ as a function of the multiplicity difference ζ assuming $m_c=26$, over a limited range of ζ. Power law fits are shown for both the gas and liquid phases to define the exponent γ, Eq. (7).

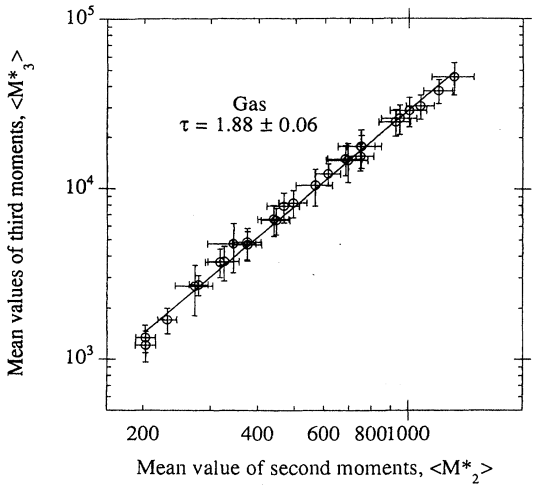

FIG. 22. Correlation between mean second and third moments, $\langle M_2^* \rangle$ and $\langle M_3^* \rangle$, for the gas phase and assuming $m_c=26$. A power law fit is shown to define the exponent τ, Eq. (9).

reduces γ to 1.03 ± 0.22. In no case is γ_{liquid} close to γ_{gas}, which implies that the conditions for a phase change have not been satisfied. No better match can be found for $m_c=30$, and it is clear that the quality of our data cannot justify an attempt to refine these estimates of m_c much further.

If we disregard the failure to confirm the presence of a phase change, one can continue the analysis as follows. The exponent β in Eq. (8) can be determined by considering the liquid phase, where Z_1 is well defined. Figure 21 shows $\langle Z_1 \rangle$ as a function of $|\zeta|$, and it can be seen that there is a power representation over a wide range of values of ζ. The value obtained for β, of 0.19 ± 0.02, with a large reduced $\chi^2=3.1$, is not in good agreement with that of 0.29 ± 0.02 reported at 1.0A GeV [9]. Here, again, the value obtained for an exponent is sensitive to the range of values chosen for ζ. Adding just one value at a higher ζ changes β to 0.24 ± 0.02, but with a still higher reduced $\chi^2=4.0$. The exponent τ in Eq. (9) can be determined from the slope of $\ln(\langle M_3^* \rangle)$ vs $\ln(\langle M_2^* \rangle)$, using only the gas phase [20]. Figure 22 shows a power law fit with $\tau=1.88\pm0.06$ and a reduced χ^2 of 0.16, with τ significantly smaller than the value of 2.25 predicted in infinite percolation models [23]. or the values reported for the 1.0A GeV data, or with the value of 2.26 calculated from our measured values of β and γ_{gas} using Eq. (10). Reducing the range of ζ values used for this fit does not make any significant change in the deduced value of τ. These results are significantly inconsistent with those reported at lower energies, suggesting that percolation theory becomes a less satisfactory representation of the breakup for these high energy interactions than it was at lower energies. Clearly it would be of great interest to repeat such an analysis, preferably with better statistics, at some intermediate energy.

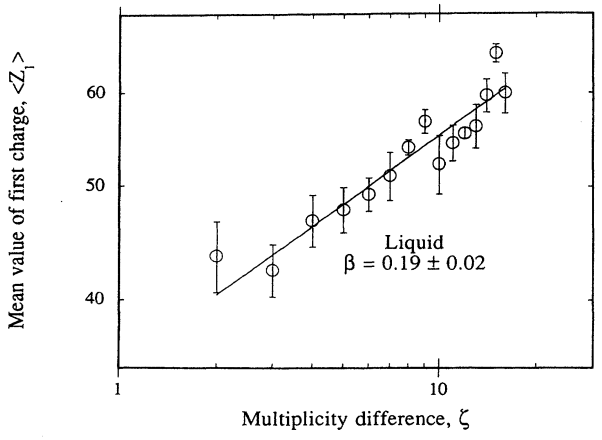

FIG. 21. Mean value of the heaviest charge, $\langle Z_1 \rangle$, as a function of ζ in the liquid phase, assuming $m_c=26$. A power law fit is shown to define the exponent β, Eq. (8).

VI. CONCLUSIONS AND SUMMARY

The fragmentation and multifragmentation of energetic heavy projectiles can be studied using nuclear emulsions, if care is taken to ensure that the samples used have high detection efficiencies. Even though this technique involves the study of interactions in a wide range of targets, multifragmentation, when expressed in terms of Z_b, appears to be relatively insensitive to the nature of the target, and the results can be compared with those obtained from studies using pure targets.

The multiplicities of multiply charged fragments reach a maximum for interactions in which approximately half the charge of the projectile remains in a bound form. Interactions with more bound charge tend to result in most of the charge remaining in a single massive fragment. Those with less bound charge simply lack enough charge to make many fragments. The majority of the multiply charged fragments are helium nuclei, while the majority of those fragments with $Z\geq3$ are light.

Multifragmentation does not appear to be strongly dependent on the energy of the projectile between 0.6A and 10.6A

GeV. Any residual energy dependence that may be present might be identified if the ALADIN and EOS data were expressed in a form that could be compared directly with our high energy results. However, the different biases between these various experiments might hinder such comparisons. Attempts to use our data to duplicate the analyses at lower energies lead to significantly different values of the various parameters and are inconclusive.

A study of the multiplicities suggests that there could be a phase change in the residual nucleus that depends on the multiplicity of the charge fragments, in a manner similar to that predicted by theories such as percolation that describe the process of multifragmentation. However, the analysis for a critical point and a phase change based on our high energy data gives results that lack internal consistency and are inconsistent with the analysis reported for the low energy results. The presence of a phase change is not established from our data.

ACKNOWLEDGMENTS

Dana Beavis and the staff of the Brookhaven National Laboratory AGS made this exposure possible. This work was partially supported in the U.S. at the University of Minnesota by DOE Grant No. DOE-FG02-89ER40528 and at Louisiana State University by grants from the NSF, Nos. PHY-89070660, PHY-921361, and INT-8913051, and in Poland by a State Committee for Scientific Research Grant No. 2P03B18409.

[1] C. J. Waddington, Int. J. Mod. Phys. E **2**, 739 (1993).
[2] R. Holynski, Nucl. Phys. **A566**, 191c (1994).
[3] M. L. Cherry *et al.*, Z. Phys. C **62**, 25 (1994).
[4] C. F. Powell, P. H. Fowler, and D. H. Perkins, *The Study of Elementary Particles by the Photographic Method* (Pergamon, London, 1959).
[5] M. L. Cherry *et al.*, Z. Phys. C **63**, 549 (1994).
[6] C. A. Ogilivie *et al.*, Phys. Rev. Lett. **67**, 1214 (1991).
[7] C. J. Waddington and P. S. Freier, Phys. Rev. C **31**, 388 (1985).
[8] P. Kreutz *et al.*, Nucl. Phys. **A556**, 672 (1993).
[9] M. Gilkes *et al.*, Phys. Rev. Lett. **73**, 1590 (1994).
[10] A. S. Hirsch *et al.*, in Proceedings of the Corinne II Workshop, 1994, LBL Report No. 36165, 1994.
[11] H. G. Ritter *et al.*, in Proceedings of the 5th Interactions Conference on Nucleon-Nucleon Collisions, 1994, LBL Report No. 36105, 1994.
[12] W. Heinrich, E. Winkel, G. Rusch, J. Dreute, and B. Wiegel, in Proceedings of the Interactions Workshop XXII, 1994 (unpublished).
[13] G. Singh and P. L. Jain, Phys. Rev. C **49**, 3320 (1994).
[14] L. Y. Geer, J. Klarmann, B. S. Nilsen, C. J. Waddington, W. R. Binns J. R. Cummings, and T. L. Garrard, Phys. Rev. C **52**, 334 (1995).
[15] L. Y. Geer, Ph.D. thesis, Washington University, St. Louis, 1994.
[16] C. J. Waddington, W. R. Binns J. R. Cummings, T. L. Garrard, B. W. Gauld, L. Y. Geer, J. Klarmann, and B. S. Nilsen, Nucl. Phys. **A566**, 427c (1994).
[17] S. E. Hirzebruch, E. Becker, H. Huntrup, T. Streibel, E. Winkel, and W. Heinrich, Phys. Rev. C **51**, 2085 (1995).
[18] W. R. Bins, T. L. Garrard, M. H. Israel, M. P. Kertzman, J. Klarman, E. C. Stone, and C. J. Waddington, Phys. Rev. C **42**, 1870 (1987).
[19] G. D. Westfall, L. W. Wilson, P. J. Lindstrom, H. J. Crawford, D. E. Greiner, and H. H. Heckman, Phys. Rev. C **28**, 1602 (1983).
[20] X. Campi, J. Phys. A **19**, L917 (1986).
[21] W. Bauer and W. A. Friedman (private communication).
[22] H. E. Stanley, *Introduction to Phase Transitions and Critical Phenomena* (Oxford University Press, New York, 1971).
[23] D. Stauffer, Phys. Rep. **54**, 1 (1979).